STRENGTH OF CONCRETE FILLED STEEL BOX COLUMNS INCORPORATING LOCAL BUCKLING

By Brian Uy,[1] Member, ASCE

ABSTRACT: Concrete filled steel box columns have recently experienced a renaissance in their use throughout the world. This has occurred due to the significant advantages that the construction method can provide. This paper deals with the strength behavior of short columns under the combined actions of axial compression and bending moment. The paper addresses the effect of steel plate slenderness limits on this behavior. An extensive set of experiments has been carried out and a numerical model developed elsewhere is augmented and calibrated with these results. A simple model for the determination of the strength-interaction diagram is also verified against both the test results and the numerical model developed in this paper. This model, based on the rigid plastic method of analysis, is existent in international codes of practice, but does not account for the effects of local buckling, which are found to be significant with large plate slenderness values, particularly for large values of axial force. Thus some suggested modifications are proposed to allow for the inclusion of slender plated columns in design.

INTRODUCTION

Concrete filled steel columns employ the use of hot-rolled steel sections filled with concrete (Oehlers and Bradford 1995; Viest et al. 1997). These columns have become popular as they speed up construction by eliminating formwork and the need for tying of longitudinal reinforcement. Current international codes such as ACI-318 and Eurocode 4 provide adequate design guidance when the component plates of the columns are typically stocky in terms of plate slenderness and if the strength of the concrete is fairly moderate (''Design'' 1994; ''Building'' 1995).

Composite columns have recently undergone increased usage throughout the world, which has been influenced by the development of high strength concrete, enabling these columns to be considerably economized. Columns designed to resist the majority of axial force by concrete alone can be further economized by the use of thin-walled fabricated steel columns (Bridge and Webb 1992). The reduced thickness of these columns has an impact on the local stability of the steel section and the compressive strength capacity of the concrete, and this has been highlighted in recent research by Bridge and O'Shea (1998), Uy (1998a), and Liang and Uy (1999) on thin-walled columns.

To consider the effects of thin steel plate in excess of compact plate slenderness limits, a thorough set of experiments has been undertaken for these types of columns. These will be described and presented herein. Furthermore, a numerical model developed elsewhere will be augmented and calibrated against the test results, with the effects of local buckling being addressed. Many previous tests have already been undertaken on composite columns with compact plate sections by other researchers; however, the tests in this paper will consider columns with very slender steel plates to allow the assessment of the effects of local buckling to be addressed.

The experiments conducted in this study include columns with both compact and noncompact steel plates. This paper will also augment an existing numerical model by incorporating the effects of local and postlocal buckling in the analysis. Fig. 1 shows the cross section of a typical composite column considered in this paper for both the experimental and theoretical studies.

[1]Sr. Lect. in Civ. Engrg., School of Civ. and Envir. Engrg., Univ. of New South Wales, Sydney, NSW 2052, Australia. E-mail: b.uy@unsw.edu.au

Note. Associate Editor: Amir Mirmiran. Discussion open until August 1, 2000. To extend the closing date one month, a written request must be filed with the ASCE Manager of Journals. The manuscript for this paper was submitted for review and possible publication on January 20, 1999. This paper is part of the ***Journal of Structural Engineering***, Vol. 126, No. 3, March, 2000. ©ASCE, ISSN 0733-9445/00/0003-0341–0352/ $8.00 + $.50 per page. Paper No. 20090.

EXPERIMENTS

To consider the effects of both concrete strength and plate slenderness, five series of columns were fabricated and constructed, with a total of 30 specimens tested. These sets of tests are categorized into individual series in Table 1. Concrete strengths used in the test specimens achieved mean compressive strengths between 32 and 50 MPa at the time of testing. Furthermore, the values of plate slenderness limits tested were between 40 and 100. The upper bound incorporates values that are far greater than plate slenderness values considered in previously tested composite columns under combined bending and compression. Compact limits for most international codes limit the slenderness values to less than 40 and thus the tests conducted herein will provide valuable results on noncompact and slender cross sections outside the realms of existing international code limitations.

Fabrication

The thin-walled concrete filled steel box columns were manufactured using steel plate of 3 mm nominal thickness and were typically composed of mild structural steel with a nominal tensile yield stress of 300 MPa. The four component plates were initially tack welded, while internal bracing was provided to minimize geometric imperfections. The boxes were then longitudinally fillet welded in a configuration illustrated in Fig. 1, and the internal bracing was removed after the welding procedure.

Testing Procedure

Experiments were conducted on columns and beams to ascertain the axial and flexural behavior of these members as well as the combined effects of bending and compression.

Columns

The column tests were conducted using a 5,000 kN capacity Denison testing machine. Experiments were carried out under displacement mode, which allowed greater control when recording the postpeak behavior. Columns under combined compression and bending were loaded with an eccentricity imposed by a knife-edge at both the top and bottom surfaces of the column. All columns were uniformly loaded by a high strength mortar plaster cast in thick steel plates at both the top

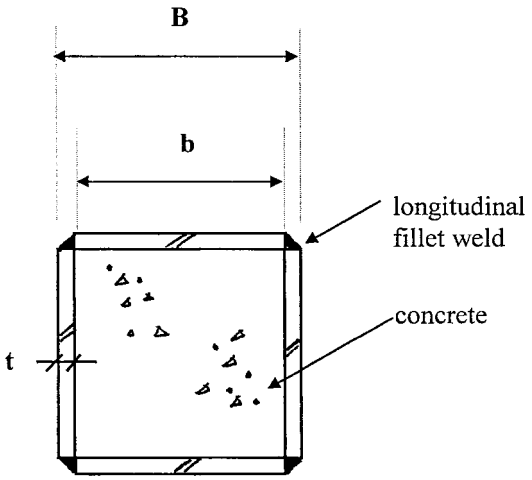

FIG. 1. Concrete Filled Steel Column Cross Section

and bottom of the column as illustrated in Fig. 2. This ensured a uniform loading surface over both the steel and concrete. In addition to the composite column tests, columns were also tested to establish their local buckling strength. These were undertaken using a different procedure where the steel was only loaded and the results have been reported elsewhere (Uy 1998a). These tests were denoted as HS5, HS11, NS5, NS11, and NS17 and have been included here for completeness. A photograph illustrating the test procedure for the axially loaded composite columns is shown in Fig. 2. A diagrammatic representation accompanies this to highlight pertinent information regarding instrumentation of the tests.

Beams

To ascertain the pure flexural strength of these sets of columns, a four-point loading beam test was carried out for each series as illustrated in Fig. 3. This beam test provided a pure flexural zone in the presence of shear.

Instrumentation

In order to study the failure modes and the behavior of the columns tested, a detailed instrumentation procedure was used. This involved the combined use of strain gauges and linear voltage displacement transducers (LVDTs) to measure the strains and deformations, respectively.

Strain Gauging

Strain gauges were used to measure strains, which allowed the assessment of curvature in the sections as well as acting as a mechanism to monitor the onset of local buckling. Each column was instrumented with between four and eight strain gauges. Fig. 2 shows the strain gauge locations and numbering scheme for the columns while Fig. 3 highlights the strain gauge locations and numbering scheme for the beam tests.

LVDTs

The use of LVDTs was employed to monitor the axial load–shortening behavior of each of the columns in question. The axial load–shortening behavior was useful in determining the peak load and assessing the ductility of a section after reaching the peak load. Figs. 2 and 3 also show the location of the LVDTs for the columns and for the beam tests, respectively. LVDTs were also used to measure the lateral deformations of the columns subjected to combined bending and compression.

Materials Testing

In order to determine the material properties for use in calibrating the numerical model, a set of materials tests was car-

TABLE 1. Experimental Data

Specimen name (1)	Series (2)	B (mm) (3)	L (mm) (4)	b (mm) (5)	t (mm) (6)	b/t (7)	f_c (MPa) (8)	f_y (MPa) (9)	N_u (kN) (10)	M_u (kNm) (11)
HS1	1	126	360	120	3	40	50	300	1,114	0
HS2	1	126	360	120	3	40	50	300	996	19.9
HS3	1	126	360	120	3	40	50	300	739	29.6
HS4	1	126	360	120	3	40	50	300	619	31.0
HS5	1	126	360	120	3	40	50	300	454	0
HS6	1	126	1,800	120	3	40	50	300	0	27.9
HS7	2	156	450	150	3	50	50	300	1,708	0
HS8	2	156	450	150	3	50	50	300	1,426	35.7
HS9	2	156	450	150	3	50	50	300	1,203	60.2
HS10	2	156	450	150	3	50	50	300	959	57.5
HS11	2	156	450	150	3	50	50	300	490	0
HS12	2	156	2,250	150	3	50	50	300	0	42.4
NS1	3	186	540	180	3	60	32	300	1,555	0
NS2	3	186	540	180	3	60	32	300	1,069	39.6
NS3	3	186	540	180	3	60	32	300	1,133	63.4
NS4	3	186	540	180	3	60	32	300	895	75.2
NS5	3	186	540	180	3	60	32	300	517	0
NS6	3	186	2,700	180	3	60	32	300	0	62.6
NS7	4	246	720	240	3	80	38	300	3,095	0
NS8	4	246	720	240	3	80	38	300	2,255	108.2
NS9	4	246	720	240	3	80	38	300	1,900	140.6
NS10	4	246	720	240	3	80	38	300	1,279	127.9
NS11	4	246	720	240	3	80	38	300	563	0
NS12	4	246	3,600	240	3	80	38	300	0	103.5
NS13	5	306	900	300	3	100	38	300	4,000	0
NS14	5	306	900	300	3	100	38	300	4,253	0
NS15	5	306	900	300	3	100	38	300	4,495	0
NS16	5	306	900	300	3	100	38	300	4,581	0
NS17	5	306	900	300	3	100	38	300	622	0
NS18	5	306	4,500	300	3	100	38	300	0	153

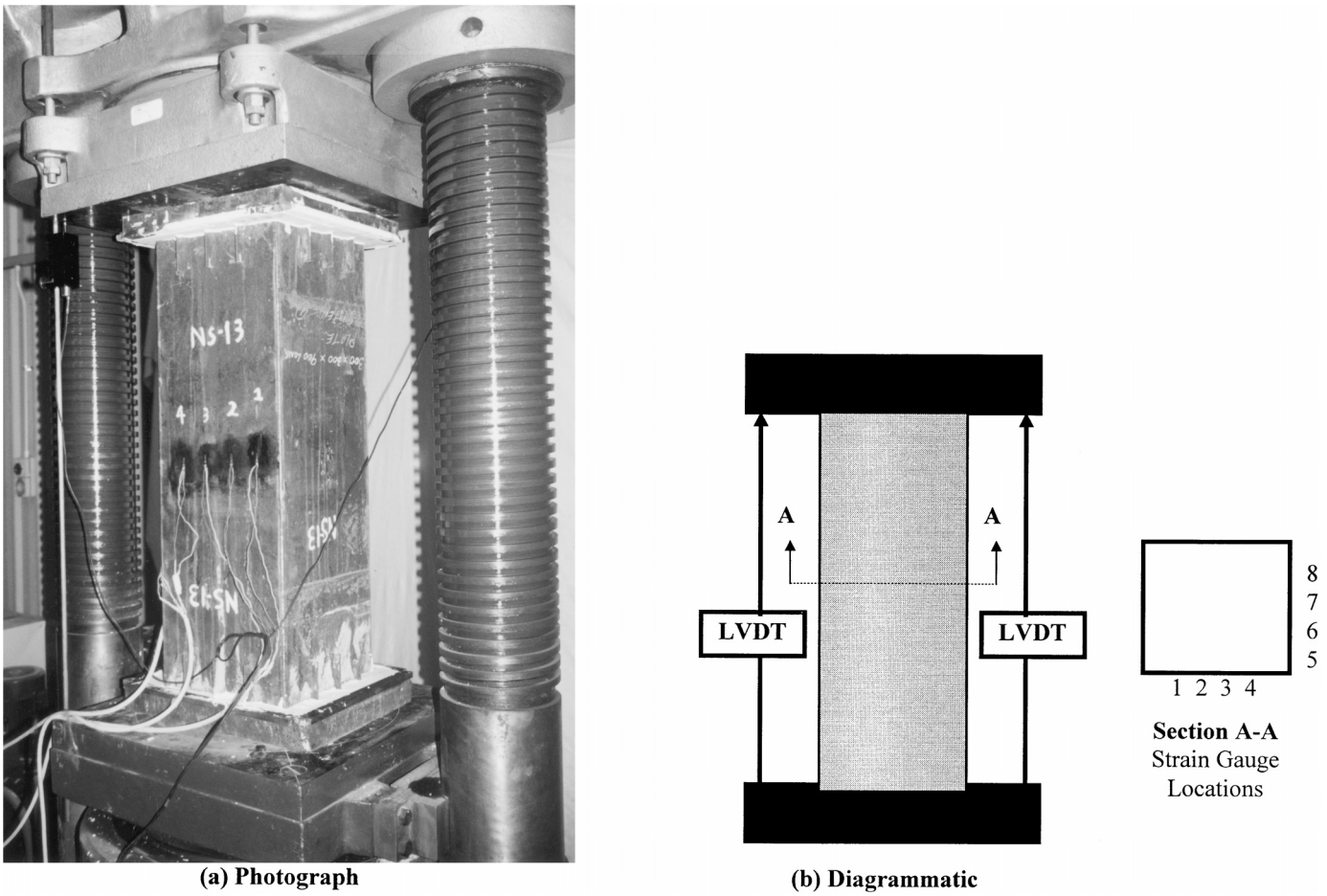

FIG. 2. Testing Procedure of Axially Loaded Columns

ried out for both the concrete and the steel used in the specimens.

Concrete

A series of concrete cylindrical specimens were cast and tested to determine the mean compressive strength of the concrete. These cylinders were tested at successive stages prior to the testing of the columns. Cylinders were also tested on the day of testing the column and beam specimens in order to ascertain the mean strength of the concrete. Table 1 summarizes the mean compressive strengths of tested cylinders of each series of tests.

Steel

The columns were fabricated using a series of plates manufactured with mild structural steel of 300 MPa nominal yield stress. Coupon tests were carried out to determine the tensile yield strength and elastic modulus. Table 1 summarizes the mean values of yield stress determined from the coupon tests for each series.

Furthermore, the compressive residual stresses were measured, and these are summarized in Table 2. The procedure for measuring the residual stresses was to apply strain gauges to the component plates of the steel box prior to welding. The strains were recorded before and after welding, and the residual strains were taken as the difference. These residual strains were measured across the full width of the component plates to give a full indication of the variation. The residual stresses were computed from the resultant residual strains, using the simplified stress-strain diagram obtained from the tensile coupon tests (Uy 1998a).

RESULTS

The pertinent measurements extracted from the experiments included axial load–shortening and axial load–strain results. Furthermore, selected specimens were cut open after testing to observe the failure modes of the concrete and the steel surfaces.

Axial Load–Shortening

The axial load–shortening results were plotted and compared for each series of tests, and these are given in Fig. 4. The results show that for columns tested under pure axial load, the peak load reduced fairly rapidly, whereas for those columns where bending was present, the reduction was less dramatic. Furthermore, the postpeak behavior of the composite column was much more brittle than that for the steel only loaded columns. This has implications on capacity reduction factors for Load and Resistance Factor Design (LRFD) philosophies currently adopted in the United States and throughout the world. Capacity reduction factors for steel columns throughout the world have been typically calibrated for axial compression at 0.90, whereas those for reinforced concrete columns are much lower at 0.60. The more brittle nature of the column tests illustrated in these tests suggests that capacity reduction factors for composite columns with slender plates may be somewhat less than 0.90. An alternative approach would be to use a mixed capacity reduction factor for the steel and concrete, respectively.

Series 3 shows the results of columns tested under pure compression as well as combined bending and compression. NS1 represents a column tested under pure compression and thus it has the highest load carrying capacity. The eccentricity

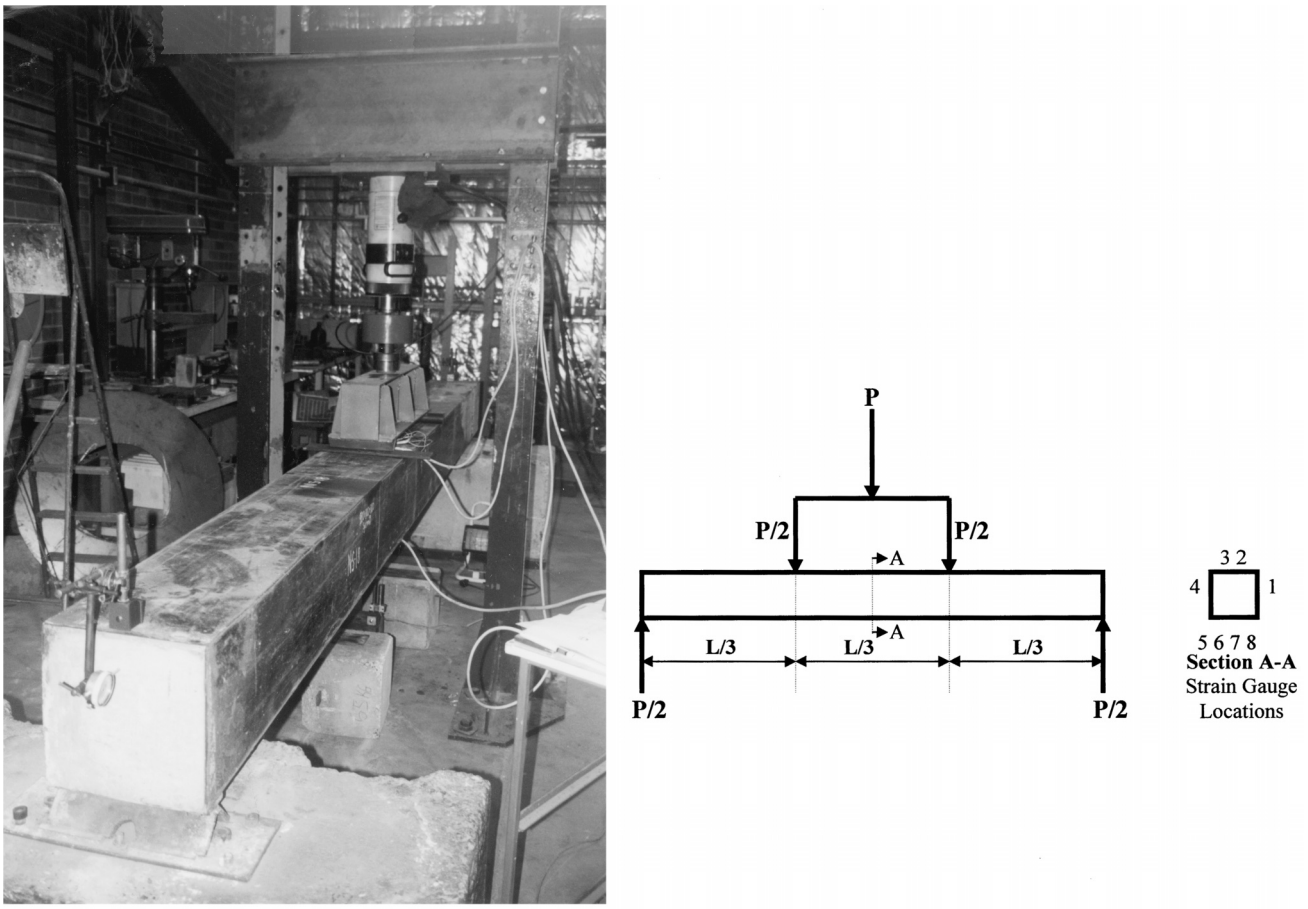

(a) Photograph (b) Diagrammatic

FIG. 3. Testing Procedure of Beams

TABLE 2. Residual Stresses

Yield stress σ_y (MPa) (1)	Average test specimen b/t (2)	Average measured residual stress σ_{res}/σ_y (3)
300	40	0.15
300	50	0.16
300	60	0.18
300	80	0.19
300	100	0.15
—	—	[mean = 0.166]

increases for columns NS2, NS3, and NS4 and this thus reduces the ultimate load able to be resisted. NS5 represents the load-deflection response of the column where the steel was loaded only in axial compression. Thus, the concrete is very influential in resisting axial load in this case. The contribution of strength is therefore 1,000 and 500 kN for the concrete and steel components, respectively. Similar behavior is evident for other series, as illustrated in Fig. 4.

Load-Deflection

An important measurement to illustrate the behavior of a beam is the load-deflection response. The load-deflection response for each of the beams tested is illustrated in Fig. 5. These curves indicate the point of yielding, the maximum load and moment, and the ductility of the member. Fig. 5 illustrates that all beam members had a significant yielding plateau, thus illustrating the ductility of these members under static flexural loading. This is quite important as these columns are essentially unreinforced, but the external steel casing prevents premature spalling and crushing of the concrete to provide very ductile behavior that is superior to a reinforced concrete column with closely spaced ties.

Axial Load–Strain

The axial load–strain results provide very useful information on axial stiffness, yielding, and the failure mechanism of the columns. Furthermore, for the specimens with large plate slenderness ratios, the strain results provide useful information on both the local and postlocal buckling behavior of the component plates. A typical axial load–strain diagram for an axially loaded column and beam is illustrated in Figs. 6(a and b), respectively.

Column NS7 was a composite column loaded in pure compression. The strain gauges SG1 through SG8 show a very similar response. Initially there is tension developed in some of the gauges, and this is due to the plaster settling and the column adjusting itself to be loaded uniformly. The strain gauges exhibit a faily linear response up until the load reaches 3,000 kN. At this load, concrete crushing occurs, which causes a significant redistribution of stress to the steel. This redistribution then promotes local buckling of the steel, which is illustrated by the erratic behavior of each of the gauges after the peak load is reached.

Specimen NS6 represents a column tested under pure flexural loading. Strain gauges SG2 and SG3 represent the extreme compressive fiber strains. One can see that these are very consistent for all stages of loading. Strain gauges SG1 and SG4 were placed as close as possible to the theoretical neutral axis. These strains gradually increased once concrete

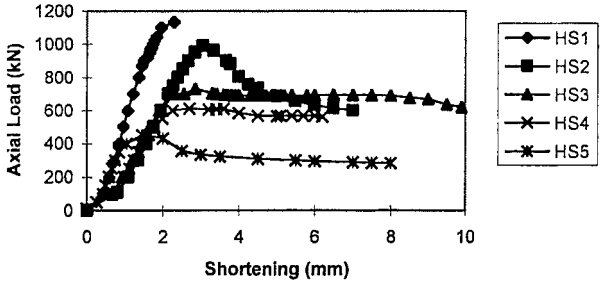

(a) Series 1 (b/t=40; f_c=50 MPa)

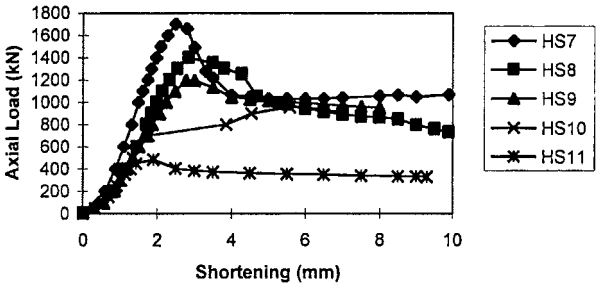

(b) Series 2 (b/t=50; f_c=50 MPa)

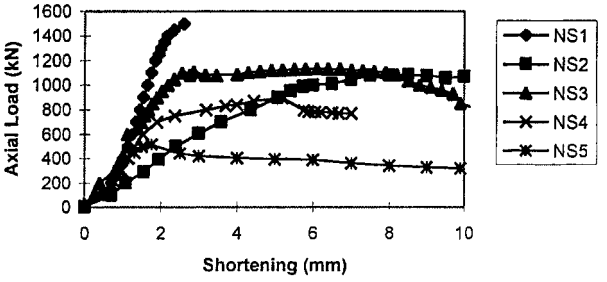

(c) Series 3 (b/t=60; f_c=32 MPa)

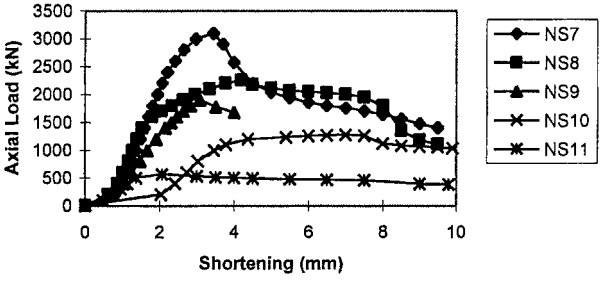

(d) Series 4 (b/t=80; f_c=38 MPa)

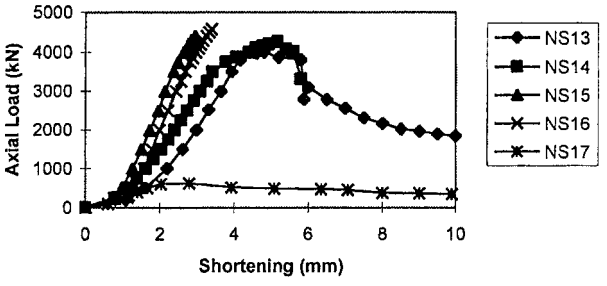

(e) Series 5 (b/t=100; f_c=38 MPa)

FIG. 4. Axial Load–Shortening Curves of Series 1–5

crushing occurred. Finally, strain gauges SG5 to SG8 represent the strains on the extreme tensile fiber. Each of these gauges is very similar in behavior, and yielding is evident once the gauges reach a value of strain on the order of 1,500 με.

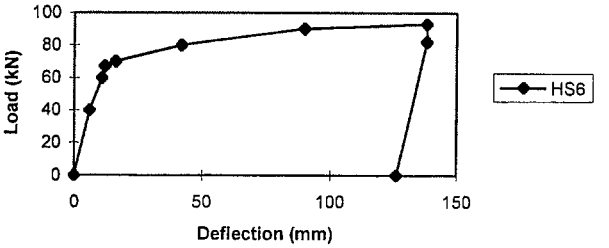

(a) Series 1 (b/t=40; f_c=50 MPa)

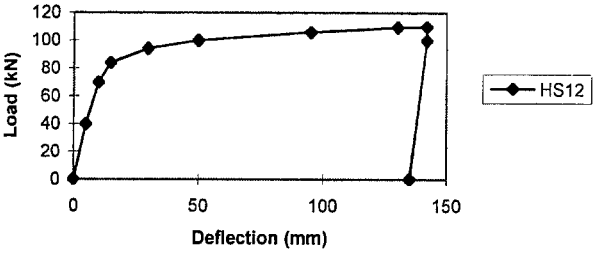

(b) Series 2 (b/t=50; f_c=50 MPa)

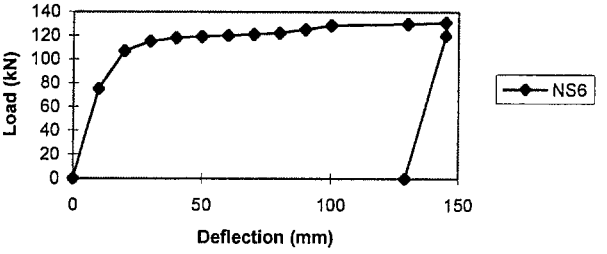

(c) Series 3 (b/t=60; f_c=32 MPa)

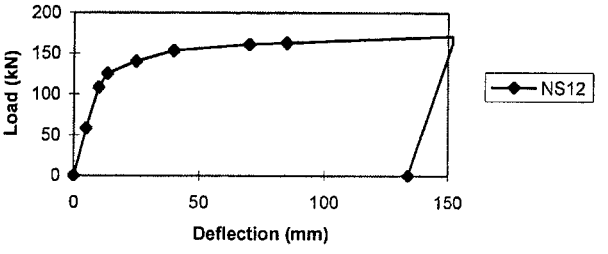

(d) Series 4 (b/t=80; f_c=38 MPa)

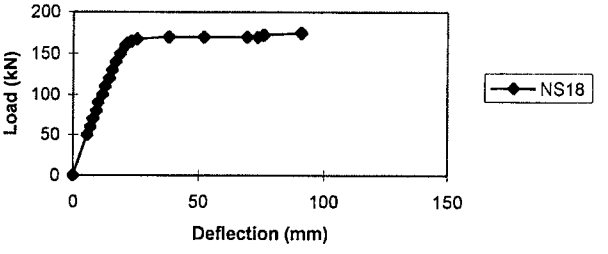

(e) Series 5 (b/t=100; f_c=38 MPa)

FIG. 5. Load-Deflection Diagrams for Beams in Series 1–5

Failure Modes

The failure modes of the columns and beams, which are of considerable importance, are primarily associated with steel yielding, steel local buckling, and concrete crushing, which were monitored for a selection of test specimens.

Columns

Each column failed in a primary compressive manner where crushing on the extreme compressive side preceded yielding

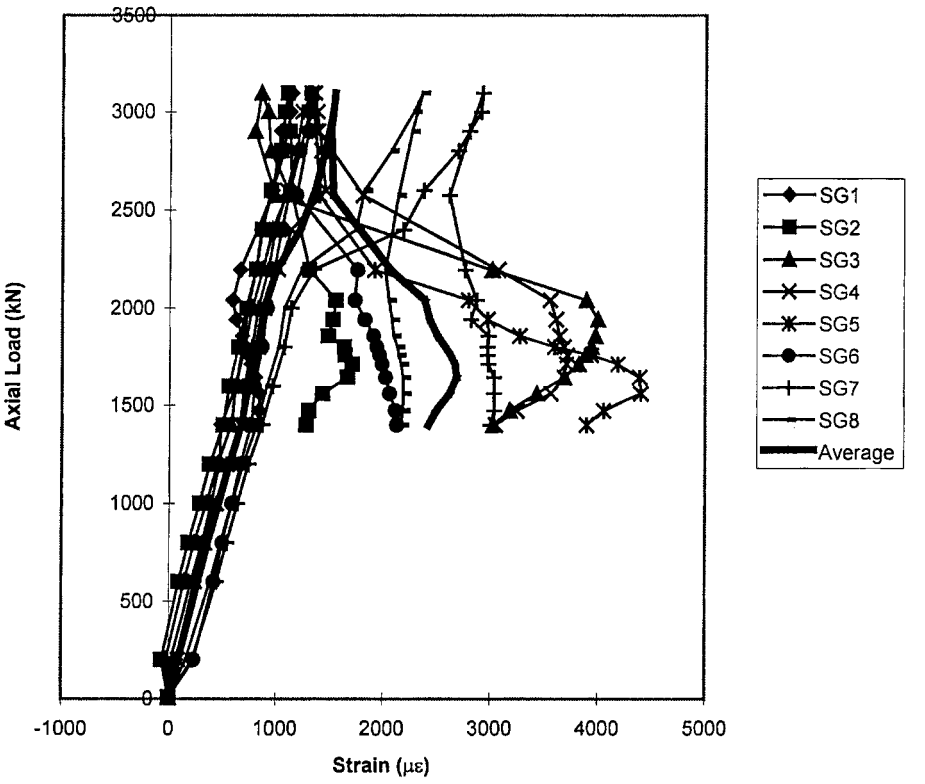

(a) NS7 (Pure Axial Load - Series 4)

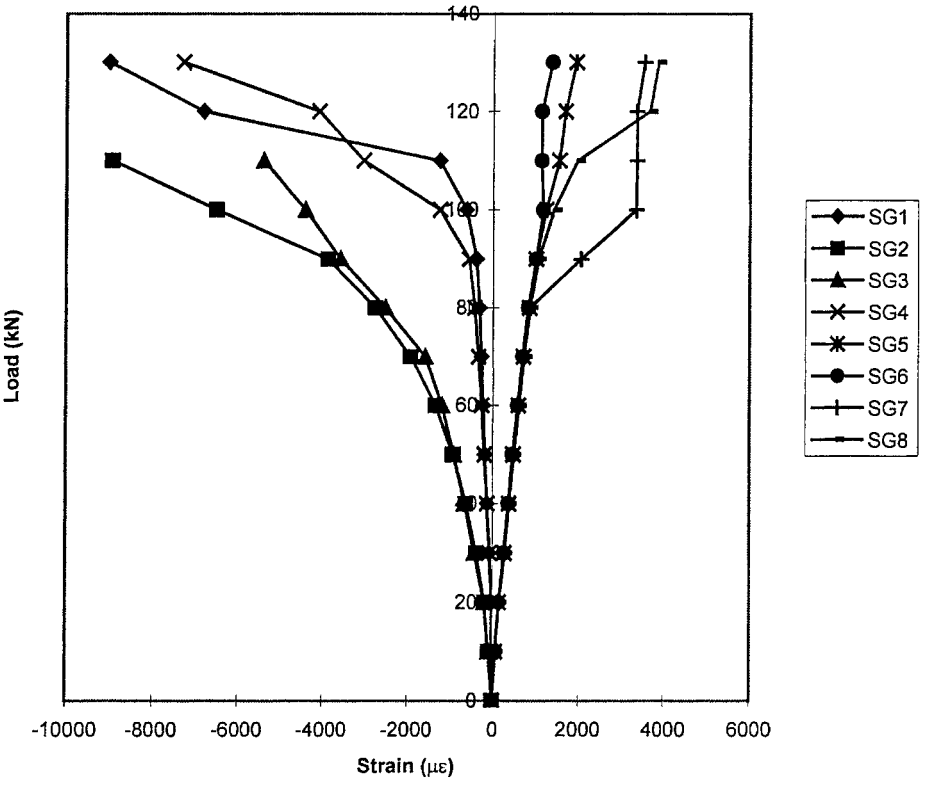

(b) NS6 (Pure Bending - Series 3)

FIG. 6. Axial Load–Strain Diagrams

in the tension region. This failure mode was initiated by concrete crushing and followed by local buckling of the steel component plates. Greater eccentricities of load may have produced failures that were primary tensile in nature, but these would have been physically impossible to achieve without fabricating an additional loading device to produce an eccentricity greater than half the column width. A photograph of a typical failed column is shown in Fig. 7.

(a) Axially Loaded Column Failure

(b) Concrete Crushing

FIG. 7. Failure of Column

Beams

All beam specimens were designed to behave in a purely flexural manner. Primary tension failure occurred in all beams and a plastic hinge formed with local buckling of the uppermost compression flange being dominant. These were all very ductile failures, which highlighted the excellent performance of this column type at overload conditions. A photograph of one of the five beams tested is shown in Fig. 8.

NUMERICAL MODEL

To predict the strength of the beams and columns, a simple model for the pure axial strength and combined bending and axial compressive strength will be presented. These methods will be calibrated here with the test results presented and compared with existing methods of rigid plastic analysis outlined in international codes of practice.

Axial Strength Model

For the columns tested in pure compression an axial strength model has been suggested for the ultimate compressive strength where

$$N_u = f_c A_c + f_y A_{se} \tag{1}$$

where A_{se} represents the effective steel area. This effective

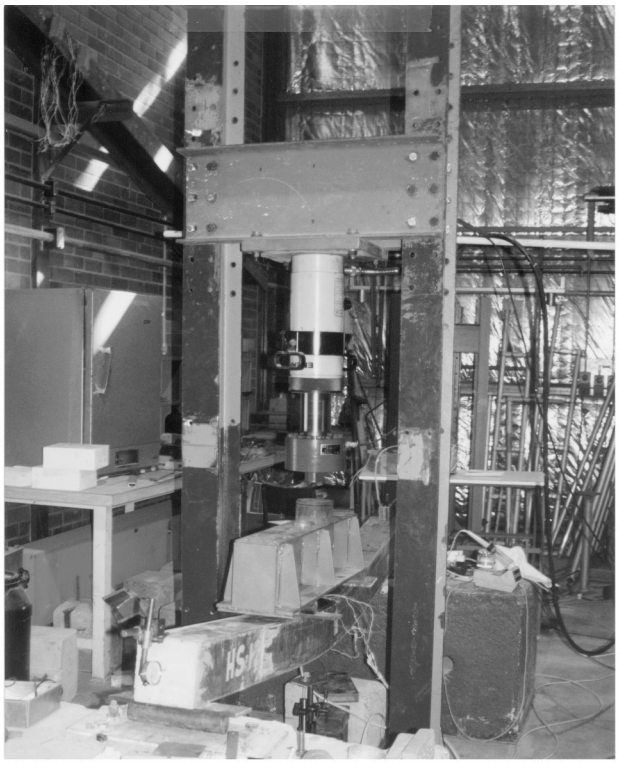

(a) Beam at Failure

(b) Plastic Hinge and Compression Flange Local Buckling

FIG. 8. Failure of Beam

steel area depends on an effective width model illustrated in Fig. 9 and given by

$$\frac{b_e}{b} = \alpha \sqrt{\frac{\sigma_{ol}}{\sigma_y}} \tag{2}$$

where $\alpha = 0.65$ according to the Australian Standard AS4100 (''Steel'' 1990), and this was found to provide a very good calibration to the test results of Uy (1998) for high plate slenderness limits. The results for all axially loaded column tests are presented in Table 3 and the mean value between test and theory has been calculated as 1.00. There exists one anomaly and unconservative result for column NS1; this can be attributed to inadequate compaction of the concrete in the column or insufficient cylinder samples for assessment of the mean compressive strength.

Now the above model for axial strength assumes one can utilize the full compressive strength of the concrete cylinder. This will be shown to be appropriate for calibration with the test results. However, one should bear in mind that these columns were tested under short-term loads. The 0.85 factor currently existent in international codes for reinforced concrete considers the effects of creep and shrinkage for long term loading. This has been shown to be lower in composite columns by Terrey et al. (1994), and thus until further results are available on strengths of columns that have been subjected to long

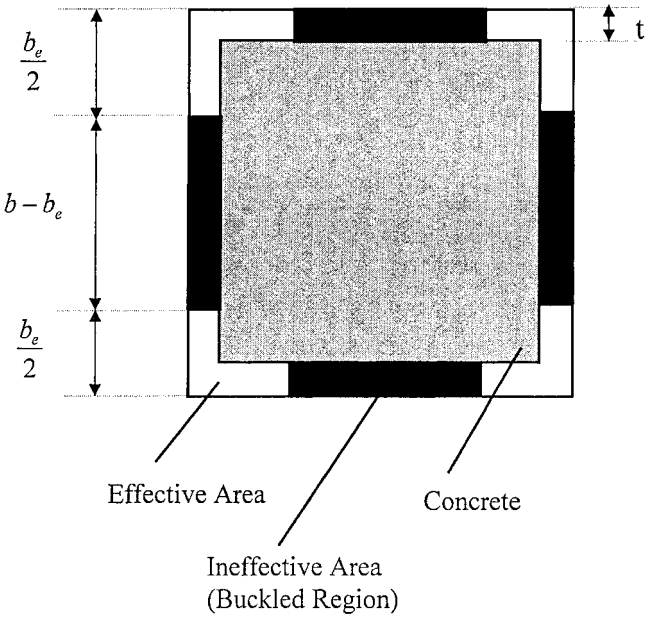

FIG. 9. Effective Width of Concrete Filled Steel Box Column

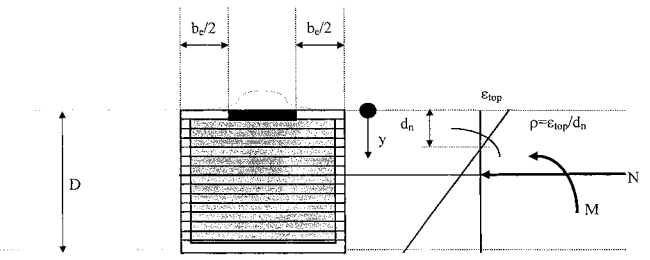

FIG. 10. Method of Slices Incorporating Local Bucking

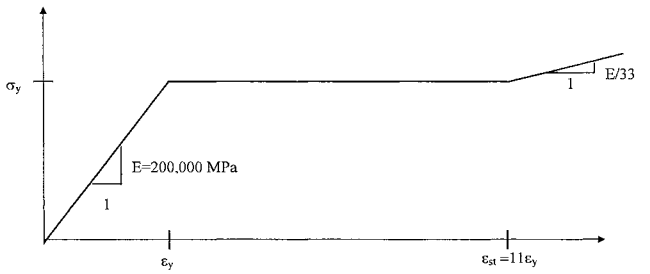

FIG. 11. Mild Structural Steel Stress-Strain Curve

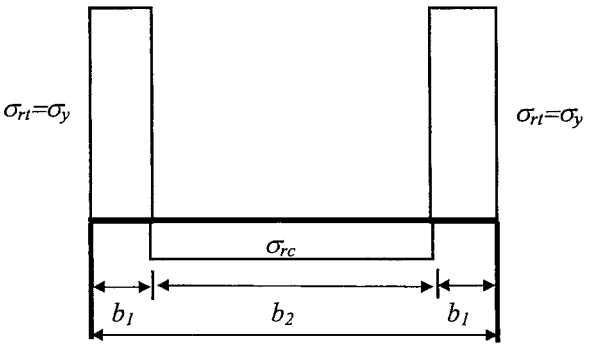

for $\sigma_{rc}=0.17\ \sigma_y$

$b_1=0.075b$

$b_2=0.85b$

FIG. 12. Residual Stress Distributions

term loads it could be suggested that this factor remains for the purposes of conservatism in design.

Combined Bending and Compression Model

In order to compare the test results for the case of combined bending and compression, a numerical model augmented and developed in a previous paper is used. This model is based on that of Uy (1996) and is calibrated with the test results. The major issue involved in the calibration is the assumption of the maximum stress for the compressive block. The method of analysis will be fully detailed herein and calibrated with the test results. The model will then be compared with existing code approaches and suggested modifications will be made. The method is based on using a series of finite slices throughout the depth of a cross section as illustrated in Fig. 10.

Steel Stress-Strain Relationship

The analysis considered in this paper is concerned with mild structural steel. The idealized stress-strain curve used in this paper assumes an elastic linear range, plastic range, and strain-hardening region, which is illustrated in Fig. 11.

Residual Stress Distributions

Residual stress distributions were based on the measured results shown in Table 2. A typical idealized residual stress distribution is shown in Fig. 12, which assumes the level of residual compressive stress to be about 17% of the yield stress. This then identifies the regions of tensile residual stress as b_1 and compressive residual stress as b_2. The level of residual stresses in welded box columns has been summarized by Uy (1998a). A maximum level of 30% of the yield stress in the compression zone was found to be a maximum based on available published data. The effects of these residual stresses were established in a parametric study by Uy (1998b). This research showed that residual stresses cause a slight increase in stiffness in the elastic range, but the ultimate strength is not affected. The presence of residual stresses did, however, cause an increase in the ultimate curvature obtained from the parametric study.

TABLE 3. Axially Loaded Column Calibration

Test number (1)	$N_{u.test}$ (kN) (2)	$N_{u.theory}$ (kN) (3)	f_c (MPa) (4)	f_y (MPa) (5)	b_c/b (6)	b/t (7)	$N_{u.test}/N_{u.theory}$ (8)
HS1	1,133	1,163	50	300	1.0	40	0.97
HS7	1,700	1,676	50	300	1.0	50	1.01
NS1	1,500	1,696	32	300	1.0	60	0.88
NS7	3,095	2,749	38	300	0.64	80	1.13
NS13	4,000	3,976	38	300	0.51	100	1.01
—	—	—	—	—	—	—	[mean = 1.00]

Concrete Stress-Strain Relationships

To model unconfined concrete, the CEB-FIP (''International'' 1970) model was used as is shown in Fig. 13. It is considered appropriate to have a descending softening branch to allow for the proper inclusion of local buckling, particularly for large plate slenderness limits where local buckling may not allow sufficient confinement. Research by Hajjar and Gourley (1996) and Zhang and Shahrooz (1999) has shown that confinement can be included to obtain both an increased strength and ductility of concrete filled steel columns. However, these studies were based on composite columns with compact plates where local buckling is inelastic. The steel plates in this study were subjected to elastic local buckling and thus separation of the steel and concrete occurs prior to the peak concrete strain being reached. This would then eliminate the possibility of confinement occurring as the Poisson's ratio of the steel would be much greater than that of the concrete, thus ensuring no transverse effects would be developed to create confinement. This is consistent with the stress-strain curves suggested in the model presented by Hajjar and Gourley (1996) where no significant confinement is available for b/t ratios greater than 40. Since the minimum b/t ratio used in this test program was 40, confinement was therefore ignored.

Cross-Sectional Analysis

The cross-sectional analysis is similar to that of Uy (1996) and thus only pertinent points will be discussed herein, which relate to the augmentation of the model with the effects of local buckling. The method is a simple equilibrium method, where a curvature is produced on the section and the neutral axis is then determined. The neutral axis is defined by using horizontal equilibrium and the bending moment is then established. This is continued for increasing values of curvature. Successive analyses then allow the development of a strength interaction diagram for the cross section in question.

Local Buckling

Local buckling was incorporated in the model by using a finite strip method to determine the local buckling coefficient and then by adopting a postlocal buckling procedure to allow for stress redistribution after buckling. The local buckling stress is calculated using the well-known equation of Bryan (1891), where

$$\sigma_{ol} = \frac{k\pi^2 E}{12(1 - \nu^2)\left(\frac{b}{t}\right)^2} \tag{3}$$

and the local buckling coefficient k is taken as 10.31, which is a significant increase on the value for a hallow steel section, where $k = 4.0$ (Uy and Bradford 1996). Once the local buckling stress is ascertained, the ratio of local buckling stress to yield stress plays an important role in identifying the redistribution of the compression flange allowed. For higher values of slenderness limit, the amount of redistribution reduces, and the model used for determining the effective width is given as

$$\frac{b_e}{b} = \alpha \sqrt{\frac{\sigma_{ol}}{\sigma_y}} \tag{4}$$

where $\alpha = 0.65$ as for the case of pure compression.

MODEL COMPARISON WITH TESTS AND EUROCODE

The model was initially calibrated against the moment-curvature response derived from the strain gauge data of the test program. Fig. 14 illustrates the comparison of the model with the experimental moment-curvature response of column NS6 that was tested in pure flexure. This comparison shows excellent agreement in the elastic range of structural response. Once

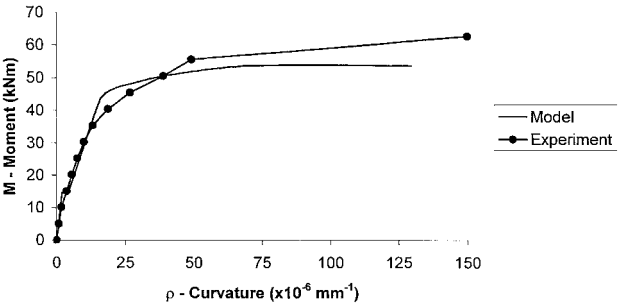

FIG. 14. Calibration of Moment-Curvature Response for NS6

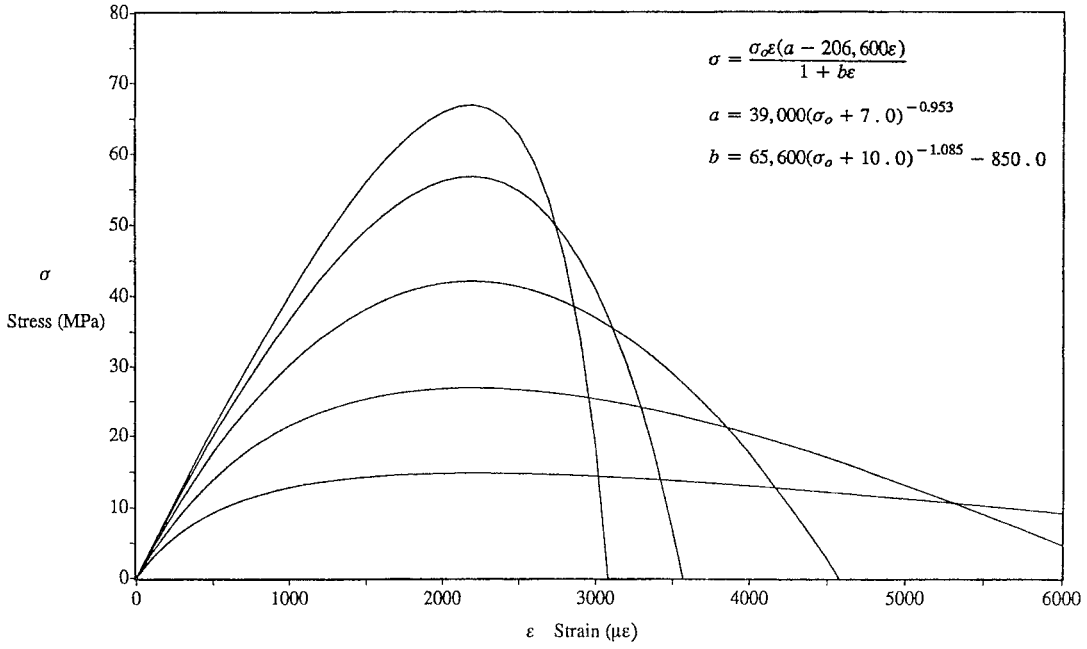

FIG. 13. CEB-FIP (1970) Stress-Strain Model

yielding begins to develop, the model slightly overestimates the stiffness; this is due to the idealized stress-strain relationship used in the analysis. The model was found to be conservative in its prediction of the peak load, as it was lower than the experimentally determined value in all cases.

The model was used to develop strength interaction diagrams for columns of the same material and geometric properties as those determined from the experimental program. Two analyses were undertaken, with the first analysis assuming no local buckling occurred in any of the component plates. This is denoted as Model. The second analysis assumed that local buckling occurred and postlocal buckling was considered as outlined in the procedure of this paper. This is denoted as Model (LB). The experimental results are also plotted for each of the test series in Fig. 15. In addition to the model, the Eurocode 4 approach has been used to ascertain strength interaction diagrams for each cross section. This approach allows the full mean compressive strength of the cylinder to be utilized, but local buckling is ignored by limiting the plate slenderness to within compact plate limits.

Series 1 consisted of columns with a *b*/*t* limit of 40, which is compact according to most international steel codes. Thus local buckling did not take place, and this is evident in the comparison for the model with and without local buckling. Eurocode 4 gave a higher strength for all points; this is partially due to the inclusion of residual stresses in the numerical analysis. Finally, the model and Eurocode 4 are all conservative for all experimental points except that for pure compression. This could be due to the maximum compression stress of the concrete being attained after local buckling of the steel occurred.

Series 2, which considered columns with *b*/*t* value of 50, exhibited very similar results for all cases. Firstly, both the numerical model and the Eurocode approach conservatively predict the strength of each of the test specimens. The differences in the model and the Eurocode 4 approach are slight but are also considered to be due to the inclusion of residual stresses in the analysis.

For Series 3, the model and the Eurocode 4 approach are conservative for the case of pure bending and for values of low axial force. However, it is the numerical model that best predicts the strength of the columns for high values of axial force. The Eurocode 4 approach is unconservative in this region as it ignores the effects of residual stresses, which have been included in the numerical analysis.

The experimental results for Series 4 are predicted well by all methods, although one experimental point close to the balance point is predicted conservatively by the numerical model, which incorporates local buckling. Since the plates of this column are slender, the numerical model incorporating local and postlocal buckling has provided a more accurate determination of the test result.

Series 5 considered columns with plate slenderness of 100. Each of the models was fairly accurate in predicting the pure bending point, although the numerical model incorporating local buckling was found to be the most conservative. For the prediction of the pure axial strength and the pure bending strength, the numerical model was found to be conservative. The model includes the effects of local buckling whereas the Eurocode approach does not. Furthermore, Eurocode 4 does not include the effects of residual stresses, which tend to reduce the strength of the section as illustrated in Fig. 15.

The comparisons show that the effects of local buckling are significant as the slenderness ratio of the steel plate is increased. The effects of local buckling are also more significant for higher values of axial force. This is due to the local buckling that occurs on more than one face as opposed to pure bending where local buckling takes place on one face only.

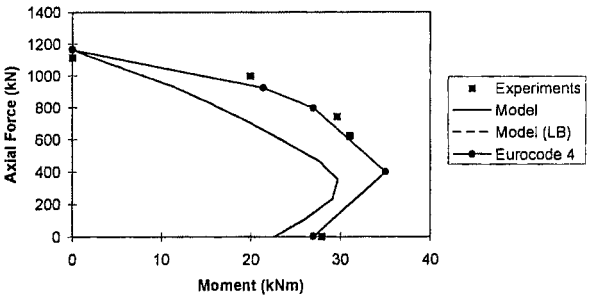

(a) Series 1 (b/t=40; f_c=50 MPa)

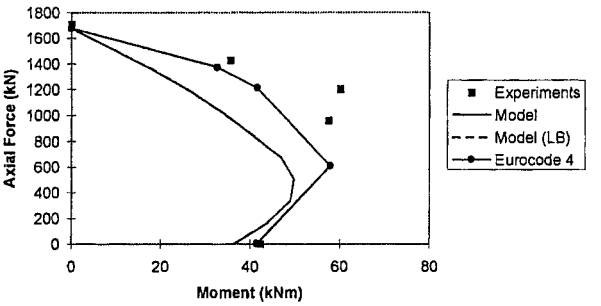

(b) Series 2 (b/t=50; f_c=50 MPa)

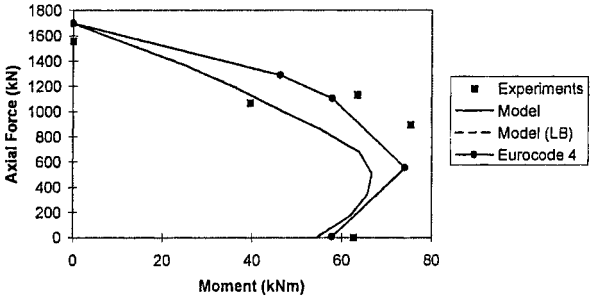

(c) Series 3 (b/t=60; f_c=32 MPa)

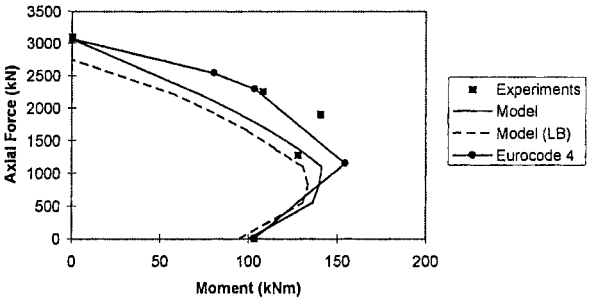

(d) Series 4 (b/t=80; f_c=38 MPa)

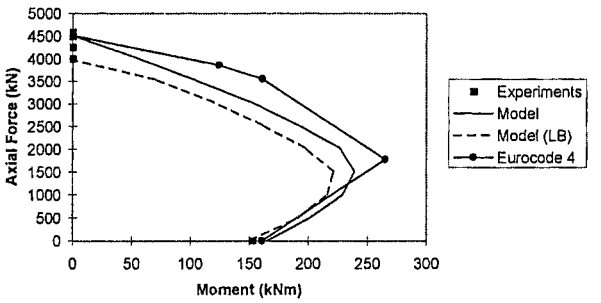

(e) Series 5 (b/t=100; f_c=38 MPa)

FIG. 15. Comparison of Experiments with Model and Eurocode 4

For values of plate slenderness in excess of 100, the reduction in strength is expected to be more severe. Thus for columns, where plate slendernesses are used in excess of compact limits, it is suggested that modifications are made to the strength interaction diagram to allow for the effects of local buckling. When applying a method such as that outlined in Eurocode 4, one can simply determine the effective width of the component plates prior to undertaking a rigid plastic analysis. This should be fairly routine for design engineers, as this approach is also required for the design of cold-formed steel structures in current international codes.

CONCLUSIONS

A set of detailed experiments has been conducted that included very large plate slenderness limits. The experiments here have shown that local buckling is significant in thin-walled composite columns. Furthermore, the use of the mean compressive stress for maximum compressive stress was found to be valid when the plate slenderness was compact. This may also be due to the good quality of concrete caused by the retention of moisture. Furthermore, since the columns were not subjected to long term loads the value of the full compressive strength may have been appropriate. However, since researchers have found both final creep and shrinkage to be much lower in composite columns than in reinforced concrete columns, the use of the mean compressive strength f_c of the cylinder may therefore be more appropriate. The effects of local buckling have been found to be significant and should be included in a modified rigid plastic analysis based on the methods of existing codes of practice where plate slenderness limits are very large. This was justified by the model presented, although international code approaches similar to Eurocode 4 can be modified to take account of this.

There is scope for further research in conducting experiments on columns with plate slenderness limits in excess of 100. Furthermore, the effect of local buckling on the slender column behavior of these types of columns for stiffness, stability, and strength will be useful contributions to further identifying the behavior of composite construction members.

ACKNOWLEDGMENTS

The writer would like to thank Ms. Cammarotto and Carusi and Messrs. Lyon and Pratsas, who have undertaken these tests as part of their undergraduate theses. Furthermore, the writer would like to thank Messrs. Bridge, Das, Laird, Liang, and Webb for their technical assistance throughout the test programme. This project was financially supported by the Australian Research Council, and this support is gratefully acknowledged. BHP Integrated Steel Division, Port Kembla, supplied the steel plate used in this project in-kind and the support of David Bare in this project is gratefully acknowledged. Finally, the writer would like to thank the reviewers of this paper for their helpful and constructive suggestions, which are reflected in the final manuscript.

APPENDIX I. REFERENCES

Bridge, R. Q., and O'Shea, M. D. (1998). "Behaviour of thin-walled steel box sections with or without internal restraint." *J. Constructional Steel Res.*, 47(1–2), 73–91.

Bridge, R. Q., and Webb, J. (1992). "Thin walled circular concrete filled steel tubular columns." *Proc., 2nd Int. Engrg. Found. Conf. of Compos. Constr.*, 634–649.

Bryan, G. H. (1891) "On the stability of a plane plate under thrusts in its own plane with applications on the buckling of the dies of a ship." *Proc., London Mathematical Soc.*, London, 22, 54.

"Building Code Requirements for Structural Concrete and Commentary." (1995). *ACI318-95; ACI318R-95*, American Concrete Institute, Detroit.

"Design of composite steel and concrete structures, part 1.1, general rules and rules for buildings." (1994). *Eurocode 4, ENV 1994-1-1*. British Standards Institution, London.

Hajjar, J. F., and Gourley, B. C. (1996). "Representation of concrete-filled steel tube cross-section strength." *J. Struct. Engrg.*, ASCE, 122(11), 1327–1336.

"International Recommendations for the Design and Construction of Concrete Structures." (1970). *Comite Europeen du Beton–Federation Internationale de la Precontrainte*, Comite Europeen du Beton.

Liang, Q. Q., and Uy, B. (1999). "Parametric study on the structural behaviour of steel plates in concrete-filled fabricated thin-walled box columns." *Ad. in Struct. Engrg.*, 2(1), 57–71.

Oehlers, D. J., and Bradford, M. A. (1995). *Composite steel and concrete structural members: Fundamental behaviour.* Pergamon, Tarrytown, N. Y.

"Steel structures." (1990). *AS4100*, Standards, Australia, Strathfield, Australia.

Terrey, P. J., Bradford, M. A., and Gilbert, R. I. (1994). "Creep and shrinkage of concrete in concrete-filled circular steel tubes." *Proc., 6th Int. Symp. on Tubular Struct.*, 293–298.

Uy, B. (1996). "Strength and ductility of fabricated steel-concrete filled box columns." *Proc., Engrg. Found. Conf., Compos. Constr. in Steel and Concrete III*, ASCE, New York, 616–629.

Uy, B. (1998a). "Local and post-local buckling of concrete filled steel welded box columns." *J. Constructional Steel Res.*, 47(1–2), 47–72.

Uy, B. (1998b). "Strength, ductility and design of fabricated thin walled steel concrete filled box columns." *Int. J. Struct. Des. of Tall Build.*, 7(2), 113–133.

Uy, B., and Bradford, M. A. (1996). "Elastic local buckling of steel plates in composite steel-concrete members." *Engrg. Struct.*, 18(3), 193–200.

Viest, I. M., Colaco, J. P., Furlong, R. W., Griffis, L. G., Leon, R. T., and Wyllie L. A. (1997). *Composite construction design for buildings.* McGraw-Hill, New York.

Zhang, W., and Shahrooz, B. M. (1999). "Strength of short and long concrete-filled tubular columns." *ACI Struct. J.*, 230–238.

APPENDIX II. NOTATION

The following symbols are used in this paper:

A_c = area of concrete;
A_s = area of steel;
A_{se} = effective area of steel;
B = column width;
b = steel plate width;
b_{se} = effective width of steel plate;
D = depth of column;
d_n = neutral axis depth;
E = elastic modulus of steel;
e = eccentricity;
f_c = mean compressive strength of concrete;
f_y = mean yield strength of steel;
k = local buckling coefficient;
L = length of column;
M = bending moment;
N = axial force;
N_u = ultimate axial force;
t = steel plate thickness;
y = lever arm;
α = factor to account for residual stresses and initial imperfections;
ε = strain;
ν = Poisson's ratio;
ρ = curvature;
σ = stress;
σ_{ol} = local buckling stress; and
σ_y = yield stress.